Available online at www.sciencedirect.com
SCIENCE DIRECT®
Polymer 45 (2004) 983–992
polymer
www.elsevier.com/locate/polymer

Glass transition and the rigid amorphous phase in semicrystalline blends of bacterial polyhydroxybutyrate PHB with low molecular mass atactic R, S-PHB-diol

S.H. El-Taweel[a], G.W.H. Höhne[b], A.A. Mansour[c], B. Stoll[d,*], H. Seliger[a]

[a]*Sektion 'chemische Funktionen in Biosystemen', University of Ulm, D-89069 Ulm, Germany*
[b]*Institut für angewandte Analysentechnik, Multscherstr. 2, D-89077 Ulm, Germany*
[c]*Department of Chemistry, Faculty of Science, Cairo University, Giza, Egypt*
[d]*Abteilung Angewandte Physik, University of Ulm, 89069 Ulm, Germany*

Received 17 August 2003; received in revised form 9 November 2003; accepted 2 December 2003

Abstract

The glass transition and the crystallinity of blends of isotactic bacterial PHB and low molecular mass atactic R, S-PHB-diols was investigated by means of differential scanning calorimetry (DSC), temperature-modulated DSC and dielectric spectroscopy. It was found that (i) T_g of crystallized blends is much lower than T_g of quenched blends, (ii) the semi-crystalline blends can only be described with a three-phase model. From the experimental results the amount of the oligomer component in the mobile amorphous as well as in the rigid amorphous phase was determined. It could be shown that the low molecular mass atactic R, S-PHB-diol is enriched in the mobile amorphous phase of the semi-crystalline blends, but 5–15% oligomer remains, however, in the rigid amorphous phase.

Keywords: Polyhydroxybutyrate; Blends; Low molecular mass atactic R, S-PHB-diols

1. Introduction

The structure of many semi-crystalline polymers could not be simply described by a conventional two-phase model consisting of crystalline and amorphous phases. About 15 years ago, the third phase, called rigid amorphous phase (RAP), an interphase between crystalline and amorphous layers, has been taken into consideration. The RAP represents a fraction of the sample that does neither contribute to the heat of fusion (crystallinity) nor to the heat capacity change (ΔC_p) or relaxation strength at the glass transition [1].

The existence of RAP in many polymers is significant and its amount can, in some cases, exceed the mobile amorphous fraction [2]. It was found, for instance, in poly (phenylene sulfide) (PPS) [3,4], polyethylene terephthalate (PET) [5–7], polytrimethylene terephthalate [8], polycarbonate PC [9,10], poly (ether–ether ketone) (PEEK) [11,12], and even in polyhydroxybutyrate PHB [10]. RAP was often associated with the existence of lamella crystals, where the crystalline lamellae are separated by very thin (20–40 Å) amorphous layers, while, on the other hand, much thicker (100–2000 Å) amorphous layers separate the lamella stacks [13,14]. It was suggested that RAP is morphologically associated with the interlamellar regions, while the normal mobile amorphous phase, which contributes to the glass transition, is associated with the larger inter-stack amorphous regions [15]. Schick et al. [10] found that in the case of PHB, and PC, (i) no change of the amount of RAP occurs in the temperature range between glass transition and crystallization and (ii) the RAP in PHB is formed during the main crystallization process [10] and not during secondary crystallization. The authors suggested that the immobilization of cooperative motions in RAP is owing to fixation of parts of the molecules to the crystallites and that this is the reason of the vitrification of the RAP. The devitrification of RAP was found to occur always far above the glass transition temperature of the mobile (normal) amorphous phase, almost nearby or during melting of the

* Corresponding author. Tel.: +49-731-502-2937; fax: +49-731-502-2958.
E-mail address: bernhard.stoll@physik.uni-ulm.de (B. Stoll).

0032-3861/$ - see front matter © 2003 Elsevier Ltd. All rights reserved.
doi:10.1016/j.polymer.2003.12.007

crystalline phase [2]. For PHB and PC Schick et al. [9,10] reported that devitrification of RAP occurs when the crystals, which were formed last, begin to melt in the lower temperature range of the endotherm.

It seems an interesting question whether the addition of plasticizer changes the properties, the composition or the size of the rigid amorphous phase. Low molar mass additives might, for instance, lower the temperature of devitrification of the RAP or even make it mobile and thus lead to a two-phase structure instead of a three-phase structure. Very few experiments are, however, reported on RAP of miscible blends [7].

As mentioned above, bacterial polyhydroxybutyrate PHB can be considered to have a three-phase structure [10]. Bacterial polyhydroxybutyrate PHB is a crystalline polyester of great technological interest, because it is a truly biodegradable and highly biocompatible polymer [16]. But it has limited industrial application, due to the restricted processing window [17] and its brittleness [18–20]. One of the main approaches to overcome these problems is to blend it with proper components [21], like poly (vinylacetate) [22], synthesized atactic polyhydroxybutyrate, R,S-PHB [23–26], oligo (R,S-PHB) diols [27], poly (epichlorohydrin) [28,29], and others [21].

This paper intends to inform about the rigid amorphous fraction of PHB-blends with low molar mass R, S-PHB-diols ($M_n = 910$, and 2670 g/mol). The use of oligomers as plasticizer is convenient, since it is known that they are miscible [27] and the glass transition temperature T_g of the amorphous oligomers is distinctly lower than that of PHB. Another advantage is that they do not evaporate or diffuse out of the sample during heating as other plasticizers do.

The blend of bacterial isotactic PHB with R, S-PHB oligomer-diol ($M_n = 1300$ g/mol) has recently been studied [27]. His results are, mainly, the following: conventional DSC measurements of this blend showed (i) one glass transition with a T_g intermediate between the T_g's of the two pure components; (ii) a decrease of the equilibrium melting point with increasing oligomer content. Using the Flory–Huggins approach the author determined a negative interaction parameter χ_{12} and concluded that the blends of bacterial PHB with oligomer R, S-PHB-OH ($M_n = 1300$ g/mol) must be miscible. However, the author gave no information about the rigid amorphous phase in this paper. According to the literature [1,2,5,9,10] the determination of the amount of RAP X_{ra} needs some experimental effort. One possibility is to measure the amount of the mobile amorphous phase X_a (e.g. from ΔC_p of the glass transition) and, in addition, the amount of the crystalline phase X_c (from the heat of fusion) and to calculate the third fraction, the amount of RAP, with

$$X_{ra} = 1 - X_a - X_c \quad (1)$$

To get reliable values of X_{ra}, we need precise measurements of ΔC_p and T_g from the mobile amorphous phase of the semi-crystallized samples. Considering the smallness of ΔC_p in partial crystallized blends, this information cannot be obtained with sufficient accuracy by conventional DSC but only by temperature modulated DSC (TMDSC). Moreover, to determine X_c we need the heat of fusion ΔH_m of the same sample and preferably from the same measurement as the ΔC_p determination to reduce the uncertainty of X_{ra} to a minimum.

2. Materials

2.1. Components

Bacterial isotactic poly (R-3hydroxybutyrate), PHB was kindly supplied by Dr Haenggi, Biomer Company, Muenchen, Germany ($M_n = 300{,}000$ g/mol, $M_w = 700{,}000$ g/mol polydispersity of ≈ 2). The PHB content is $>98\%$, the content of polyhydroxyvalerate (PHV), is $<1\%$. The remaining cell membrane and membrane lipid content is about 1%. PHB was obtained as powder and used as delivered without further purification.

The oligomer, the atactic R, S-PHB-OH (abbreviated as G2670), as well as the other oligomers of this series with $M_n > 1300$ g/mol, was prepared by ring-opening polymerisation of βbutyrolacton and butyleneglycol at 135 °C for 120 min in the presence of dibutyltinoxide as described in Ref. [30].

The oligomer, abbreviated as G910 and some others with molecular mass ranging from 600 to 1300 g/mol were prepared by transesterification of ethyl hydroxybutyrate with butyleneglycol in presence of dibutyltinoxide as catalyst. For details of this method see Ref. [31].

The structures of PHB, G910 and G2670 (see Table 1) were investigated with NMR, and ^{13}C NMR. Molecular masses and polydispersities of the samples were determined by gel permeation chromatography (GPC) using Waters pump model 510, Waters differential refractometer model 410 and Waters date module model 730 with 10^3–10^5 Å. Ultrastyragel columns connected in series. Chloroform was used as the eluent at flow rate 1.5 $cm^3\,min^{-1}$ and polystyrene was used as a standard for calibration (see Table 1).

2.2. Blends

The components, in appropriate weight ratio, were dissolved in chloroform (10% wt/v) under stirring at 70 °C. Then the solution was cast on the glass Petri dish, and the solvent was slowly evaporated at room temperature. The remaining films were then aged at least 2 weeks at room temperature, and dried in vacuum.

Table 1
Structure and molecular masses of the components of the investigated blends

Materials	Structure	M_n (g/mol)	M_w (g/mol)
PHB	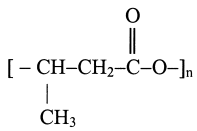	300,000	700,000
G2670	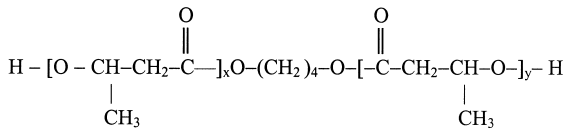	2670	4300
G910		910	1200

3. Experimental methods

3.1. Differential scanning calorimetry

Differential scanning calorimetry (DSC) measurements were performed with a Q1000 apparatus with Tzero® techniques from TA Instruments. The sample mass for these measurements was in the range from 4 to 8 mg. Samples were encapsulated in standard aluminium pans.

Temperature, heat flow and heat capacity were calibrated as usual [32] using indium and sapphire (Al_2O_3) (and in addition polystyrene) as calibrants. The temperature read out of the DSC is estimated to have an uncertainty better than ± 0.5 K. The heat flow rate calibration results in an uncertainty better than 5%.

Some samples from cast film were first heated to 200 °C at a heating rate of 10 K/min, to remove any thermal prehistory (first heating scan) and then cooled at 10 K/min to −90 °C (first cooling) and then reheated at 10 K/min from −90 to 200 °C (second heating).

The 'quenched samples' were prepared by keeping the sample pans in a drying cabinet at 200 °C for 3 min and then quickly pressing them on a cold metal plate at 0 °C. These samples were then measured in the DSC from −90 to 200 °C at 10 K/min.

The 'crystallized samples' were prepared by keeping them in the DSC at 200 °C for 3 min followed by cooling at −30 K/min, annealing at 80 °C (near to temperature of maximum growth rate, in order to achieve complete crystallization in very short time) for 3 h with subsequent cooling to −90 °C and then run in temperature modulated mode (TMDSC) [32], from −90 to 50 °C at 2 K/min (temperature amplitude = 1 K, period = 60 s). This was done to determine the relevant glass transition quantities from the 'reversing heat capacity' [32] signal. The glass transition temperature, T_g, was taken at the half height point of the specific heat step. The ΔC_p uncertainties from these TMDSC measurements are ± 0.03 J g^{-1} K^{-1}. From reproducibility tests, the uncertainty in the determination of T_g is estimated to be less than ± 1 K for samples where $\Delta C_p \geq 0.3$ J g^{-1} K^{-1} and ± 3 K for samples where $0.3 \geq \Delta C_p \geq 0.1$ J g^{-1} K^{-1}.

The relation between the glass transition determined via modulated (TMDSC) and conventional DSC experiments (with constant cooling resp. heating rate) has been discussed by Schick and co-workers [33,34] as well as in Ref. [35,36]. The authors describe an empirical equation

$$\beta = 2\pi f \Delta T \tag{2}$$

which connects the cooling rate $\beta = -dT/dt$ in conventional DSC experiments with a 'fictive frequency' f corresponding to a dynamic experiment. The empirical quantity ΔT was found to be about 15 K. Thus, equation (2) allows to assign a frequency $f = 0.0018$ Hz to our conventional DSC-experiments done at a cooling rate $\beta = -10$ K/min. The frequency of our TMDSC experiments, on the other hand, was $f = 0.017$ Hz. As the frequencies are different by one order of magnitude, there must be a difference of about 3 K between the T_g from TMDSC and T_g from conventional DSC experiments at −10 K/min cooling rate. To simplify the discussion in the present paper, we shall use the abbreviation 'T_g' for the results from conventional DSC experiments at 10 K/min. To get comparable results from TMDSC experiments we evaluated the temperature of the peak maximum of the phase signal and subtracted 3 K to get the T_g values as plotted in Figs. 7 and 8.

For determination of the heat of fusion ΔH_m of crystallized samples, these were heated to 200 °C at a heating rate of 10 K/min. The heat of fusion ΔH_m was calculated from the peak area using the TA Instrument software and a baseline, which is assumed to be linear in the region from room temperature to the melt at 200 °C. The total area above the baseline (including all the melting peaks) is taken to calculate ΔH_m. The experimental error depends on the peak size but is less that $\pm 5\%$.

3.2. Dielectric spectroscopy

Dielectric measurements were done by a Solartron impedance analyzer model 1260 from Schlumberger Technologies UK, according to the method described in Ref. [37].

The frequency range was 10^{-3}–10^{6} Hz. The sample cell was connected in different ways to the impedance analyzer, according to different frequency ranges. For the low frequency range below 100 Hz, an electrometer preamplifier was used.

The precision of the real part of the dielectric constant is dominated by the error in the measurement of the thickness of the sample, while the error in the measurements of tan δ is about 2×10^{-3} for all frequencies except 1 MHz.

The sample preparation was done by pressing at 200 °C for 3 min between stainless steel plates together with a polyimide film spacer. The thickness of the samples was about 0.1 mm and the area was 700 mm^2. Some of the samples were quenched using a cold (0 °C) metal plate, some others were crystallised at (80 °C 3 h) in the dielectric cell.

4. Results and discussion

In order to study the thermal behaviour of blends of bacterial PHB with low molecular mass atactic R, S-PHB-diols, DSC runs were performed. Fig. 1 shows DSC-cooling curves of blends of PHB with G910 crystallized from the molten state at a cooling rate −10 K/min. From these curves, some useful data can be obtained for describing the non-isothermal crystallisation behaviour of PHB and its blends, such as the peak temperature of crystallization T_c and the glass transition temperature T_g of the remaining amorphous part. As seen in Fig. 1, T_c shifts to lower temperatures when the content of G910 increases. This behaviour is known from other blends of PHB with amorphous polymers [21–29]. The authors attributed this phenomenon to two reasons: (i) the dilution of the PHB chains at the crystal growth front, and (ii) the drop of the thermodynamic crystallization driving force caused by the melting point depression of PHB in the mixture (see Fig. 2). As one example, the blend of 30% PHB with 70% G910 (Fig. 1e) does not crystallize during this cooling run at all, only on reheating at +10 K/min cold crystallization occurs (see Fig. 2e).

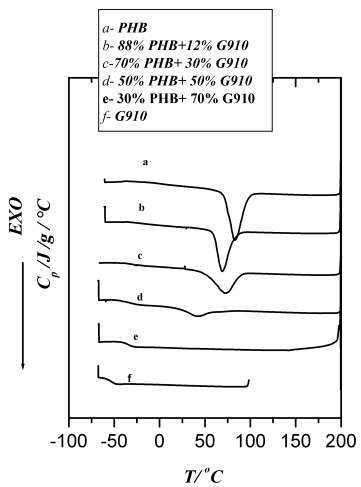

Fig. 1. DSC-cooling curves (in units of heat capacity) of blends of PHB with G910 measured at −10 K/min after 3 min at 200 °C. Curves are shifted vertically for clarity.

4.1. Glass transition

In order to get more precise information about the glass transition, the change of the specific heat capacity ΔC_p and the amount of the mobile and the rigid amorphous phase in semi-crystallized blends, temperature-modulated DSC and dielectric measurements were performed. Several measurements were done with blends of PHB with G910 and G2670 of different composition. Some examples of such TMDSC curves are shown in Fig. 3. The 'reversing part' of the specific heat capacity shows the typical step-like change at the glass temperature T_g whereas the phase signal exhibits a peak there. From comparison of Fig. 3a and b we find, as expected, that the crystallized sample has a smaller ΔC_p than the quenched sample, but the glass transition temperature T_g of the crystallized sample is much lower than that of the quenched one. This behaviour is in contrast to other semicrystalline homopolymers like polyethylene-terephthalate PET [33]. The results from TMDSC are plotted in Figs. 7 and 8.

In order to confirm these results from TMDSC with another experimental method, dielectric measurements were performed with the same blends. Fig. 4 shows the frequency dependence of the dielectric loss of the quenched blend of 75% PHB with 25% G2670 in the temperature range of the glass process. In the 5 °C curve we observe a loss peak with maximum at about 10 Hz, which is attributed

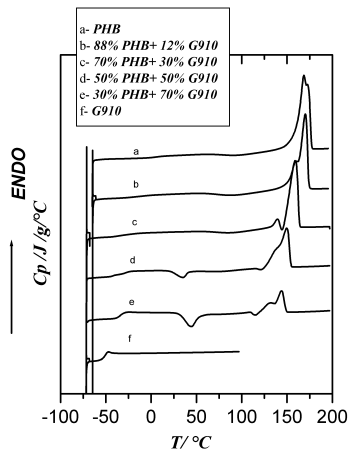

Fig. 2. DSC-heating curves (in units of heat capacity) measured at +10 K/min after the cooling procedure according to Fig. (5). Curves are shifted vertically for clarity.

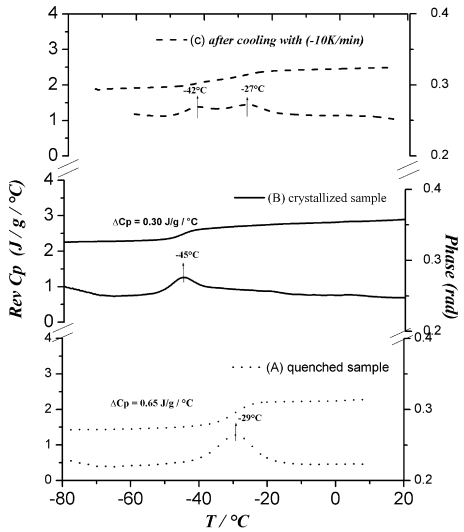

Fig. 3. TMDSC curves in the glass transition region of the 50% PHB with 50% G910 blend; upper curve: reversing C_p; lower curve: phase angle; (A) quenched sample, (B) crystallized sample (3 h at 80 °C), (C) after cooling from 200 °C with − 10 K/min.

to the glass relaxation (cooperative molecular motion in the mobile amorphous part of the sample). At frequencies lower than 0.1 Hz, we observe an increase of dielectric loss, which appears in similar form in many dielectric measurements of amorphous polymers; this is interpreted as the effect of ionic conductivity [38]. The maximum frequency f_{max} of ϵ'' can be related to a mean relaxation time τ of the molecular segments by

$$\tau = 1/(2\pi f_{max}) \quad (3)$$

At lower temperatures, this dielectric loss peak is shifted to lower frequencies, as usual (about one decade for 4 °C). This means that the relaxation time τ of molecular motions increases at lower temperatures. At the glass transition temperature T_g, τ exceeds the usual laboratory time scale.

The measurements in Fig. 5 are obtained after annealing

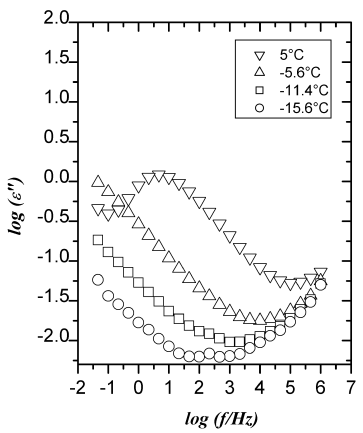

Fig. 4. Frequency dependence of the dielectric loss at different temperatures in the glass transition region of the quenched blend of 75% PHB with 25% G2670.

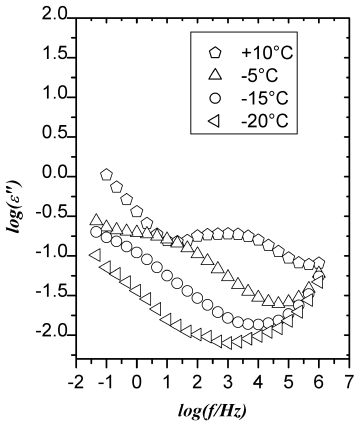

Fig. 5. Frequency dependence of the dielectric loss at different temperatures in the glass transition region of the crystallized blend of 75% PHB with 25% G2670.

of the sample from Fig. 4 at 80 °C for 3 h in order to get it well crystallized. The dielectric loss shows the same behaviour as in Fig. 4 but the peak is lower and broader. This is a normal behaviour after crystallization of polymers because of the smaller number of mobile molecules in the crystallized sample and of the constraints of their mobility in the surface region of the crystals.

If we plot the maximum frequency f_{max} for all compositions of blends of PHB with G2670 against the reciprocal temperature we get a so-called activation diagram (Fig. 6). From this figure, it is clear that at a certain temperature, f_{max} for the crystallized samples is higher than for the quenched samples of the same composition.

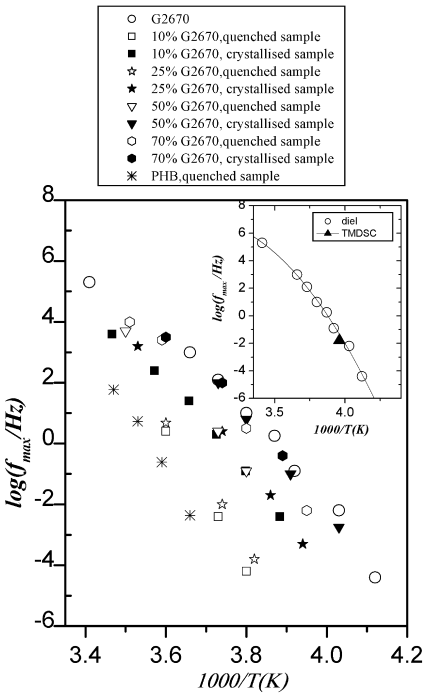

Fig. 6. Activation diagram from dielectric measurements of different quenched as well as crystallized blends of PHB with G 2670. The inset repeats the results for pure G 2670 together with one TMDSC result.

In order to compare the T_g information from Fig. 6 with the results from TMDSC measurements, we can refer to the well-known fact that the activation curves, which have been obtained from dielectric experiments, are parallel to those from TMDSC measurements for many amorphous polymers [33–36]. For instance, for polyvinylacetate (PVAC) they are very near to each other (difference only 2 K). Similar results were obtained in this work if we compare the results from TMDSC with those of the dielectric measurements (see inset in Fig. 6). Therefore, we can assume that the activation curves from calorimetric and dielectric measurements of these blends are very near to each other too. With Eq. (2), we can determine even the quasi-static glass transition temperature for cooling or heating with 10 K/min by reading the respective values from Fig. 6 at the 'fictive' frequency 0.0018 Hz. As a result, the T_g for the crystallized blend is considerably lower than for the quenched one. The same was done for blends with G910 and the results are plotted in Figs. 7 and 8. A good agreement between the results obtained from the dielectric measurements and DSC can be stated.

Quenched binary blends of PHB with G910 or G2670 showed one single glass transition between those of the two pure components, and the glass transition temperature is close to that predicated from the Fox equation [39] (see Figs. 7 and 8). Therefore, it is confirmed, that the blends of PHB with G910 and G2670 are miscible.

However, the crystallized blends show a glass transition temperature, which is significant lower than that of the quenched sample of the same composition. The reason for that is that in these blends, the crystallization of PHB leads to a change of the

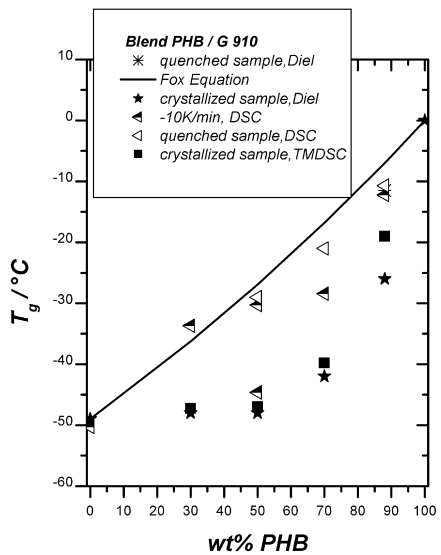

Fig. 7. Glass transition temperature in dependence on composition for quenched and crystallized blends of PHB with G910 from TMDSC, DSC and dielectric measurements. The solid line characterizes the Fox equation.

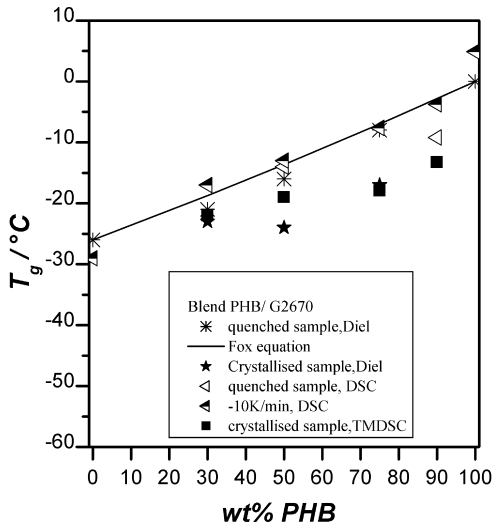

Fig. 8. Glass transition temperature in dependence on composition for quenched and crystallized blends of PHB with G2670, from TMDSC, DSC and dielectric measurements. The solid line characterizes the Fox equation.

composition of the amorphous phase, namely an enrichment of G910 or G2670 and consequently a T_g decrease. For example, for the blend of 75% PHB with 25% G2670 the T_g of the quenched sample is −7 °C, whereas that of the crystallized blend is −18 °C. According to Fox equation [39], such a T_g would correspond to a composition of 33% PHB and 77% G2670 of the mobile amorphous phase of the crystallized sample. The same behaviour also appears in the blends of bacterial isotactic PHB with G 910. For example, for the blend 70% PHB with 30% G910 T_g of the crystallized sample is −41 °C. This T_g would correspond, according to the Fox equation, to a composition 19% of PHB and 81% of G910 inside of the mobile amorphous part of the sample. The same trend was reported for the blends of PHB with atactic polyepichlorohydrin [28,29], and the blend of atactic R, S-PHB with polylactic acid [40,41].

It is interesting to note that only one glass transition was observed for all compositions and all thermal histories of the blends except for the blend of 50% PHB with 50% G910, if cooled from the melt at −10 K/min (see Fig. 3c). The two peaks in the phase signal in Fig. 3c are, however, well separated, they are almost equal in magnitude and clearly resolved. It should also be mentioned that an unusual broad glass transition (about 20 °C) has been observed for blends of 70% PHB with 30% G910 after cooling at −10 K/min which may be the sum of two overlapping glass transitions. The simplest explanation for these findings may be that the crystallization was not completed at −10 K/min (see Figs. 1 and 2), the spherulites are not volume-filling and the resulting material is a mixture of a partial crystalline and a totally amorphous blend which show different T_g's. More investigation will be done in the future to clarify this phenomenon.

4.2. Rigid amorphous phase

Schick et al. [10] have found that semicrystalline PHB must be described with a three-phase model (with a crystalline, a mobile amorphous and a rigid amorphous phase) rather than with the common two phase model. It is an interesting question to see whether this model even holds for blends, in particular miscible blends, and to determine the amount of the obvious existing rigid amorphous phase in different blends of PHB with the atactic oligomers of low molecular mass (G910 and G2670).

The fraction of the mobile amorphous phase in crystallized blends can be estimated from the ΔC_p of TMDSC curves:

$$X_a = \frac{\Delta C_p \text{ (crystallized blend)}}{\Delta C_p \text{ (completely amorphous blend)}} \quad (4)$$

where ΔC_p (crystallized blend) of the glass transition process was measured with blends which were crystallized for 3 h at 80 °C and ΔC_p (completely amorphous blend) = 0.65 J g^{-1} °C^{-1}, this is an average value from measurements of quenched PHB and the pure oligomers G910 and G2670. To take the average value for these calculations seems reasonable in this case, as the measured values turned out to differ only slightly within our experimental uncertainty and a correction relative to the oligomer content [44] does not make much sense. The respective results are plotted in Figs. 10 and 11.

It is also possible to determine the amount of the mobile amorphous fraction (at temperatures above T_g) from dielectric measurements. In the case of very low frequencies (the quasi-static case), where the molecular dipoles are able to follow the applied electric field, there is a great difference between the permittivity of the mobile amorphous phase and that of the crystal. For quenched PHB, we measured $\epsilon \approx 10$ and almost the same value was obtained for the pure oligomers. On the other hand, in the case of very high frequencies (where the dipoles are not able to orient in the alternating field and therefore behave like in the immobile phase) a value of $\epsilon \approx 3.3$ can be assumed for all blends.

The case of immobile dipoles can also be easily realized at low temperatures ($< T_g$). This way, if the level of the permittivity of the blends is measured at very low frequencies, it is possible to calculate the amount of mobile amorphous material in the sample. Since blends are heterogeneous dielectric material, with very different components, a linear interpolation is not possible and we have to use a theory of heterogeneous dielectric materials. One of the simplest equations for a two phase system (with mobile and immobile dipoles), symmetrical with respect to the two components, is reported by Böttcher [42]. It was derived for balls of material 2 embedded in a matrix of material 1:

$$\frac{[\epsilon - \epsilon 1]}{3\epsilon} = \delta 2\left[\frac{\epsilon 2 - \epsilon 1}{\epsilon 2 + 2\epsilon}\right] \quad (5)$$

where ϵ_1 and ϵ_2 are the permittivities of material 1 and 2, respectively, and δ_2 the volume fraction of material 2. ϵ is the permittivity of the heterogeneous blend. On reasons of symmetry, this equation is applicable over the whole range of composition (0–100% of material 2). Of course the morphology of the PHB blends is much more complicated than the simple model of balls in a matrix, but Eq. (5) may serve as a first approximation.

From our results, we assign material 1 ($\epsilon_1 = 3.3$) to the immobile dipoles (including the crystal and the rigid amorphous phase) and material 2 ($\epsilon_2 = 10.3$) to the mobile amorphous phase. The permittivity ϵ of the blends was measured at low frequencies from scans at selected temperatures. Inserting these values in Eq. (5), we obtained the volume fraction δ_2 of the mobile amorphous phase.

The permittivity of the blends at high temperatures and low frequencies is, of course, influenced by the Maxwell–Wagner polarisation, caused by the migration of ionic impurities. Therefore, care was taken during the evaluation of the data, to separate these effects from the contribution of the dipoles. The X_a results from dielectric experiments were added to Figs. 10 and 11 with an error bar corresponding to an uncertainty of ± 10% for these measurements.

The crystallinty X_c, on the other hand, was calculated from the melting peak in conventional DSC curves:

$$X_c = \frac{\Delta H \text{ (blend)}}{\Delta H \text{ (100\% crystalline PHB)}} \quad (6)$$

where ΔH(blend) the area of the melting peak of blends crystallized at 80 °C for 3 h and ΔH(100% crystalline PHB) = 146 J/g taken from literature [43]. Fig. 9 shows that there is a nearly linear relation between the enthalpy of fusion per gram of blend with G910, G2670 and the PHB content. In other words, the partial crystallinity of the PHB component in the blend is practically not influenced by the

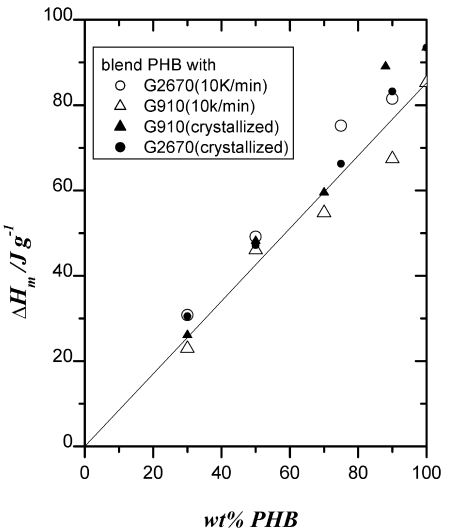

Fig. 9. Melting enthalpy in dependence on composition for different crystallized blends. The linear relationship (solid line) is obvious.

blend composition. It should be noted that every X_c is an average value from several measurements.

The resulting X_a and X_c for blends of PHB with G910 or G2670 are plotted in Figs. 10 and 11. Additionally, the respective results for pure PHB from Schick et al. [10] are included.

From Figs. 10 and 11, it follows that the sum of X_a and X_c is different from 1. This confirms the existence of a significant amount of rigid amorphous phase X_{ra} in these blends, which can be calculated according to Eq. (1):

$$X_{ra} = 1 - (X_c + X_a)$$

X_{ra} of the two types of blends is plotted in Figs. 12 and 13. From literature [2,10] it is known that at least for pure polymers, the rigid amorphous phase is strictly connected with the crystalline phase. From Fig. 9 follows that ΔH, and therefore even the crystallinity, is linear dependent on the weight fraction of PHB. So it could be expected that X_{ra} should be a linear function of the composition too. However, from Figs. 12 and 13, it is obvious that the amount of rigid amorphous fraction is non-linear dependent on the weight fraction of PHB. One possible explanation for such a non-linearity is that the rigid amorphous phase contains not only PHB but varying amounts of amorphous G910 or G2670 as well.

Now the question arises how to determine the composition of the rigid amorphous fraction in the blends. One way is to assume that the *ratio* of the amount of PHB in the rigid amorphous and in the crystal phase is unchanged for all blends. In other words, it is assumed that the amount of PHB in the RAP is proportional to the total amount. This is described by the straight line in Figs. 12 and 13. This assumption is reasonable because from literature it is known that the RAP is connected to the crystals and the amount of

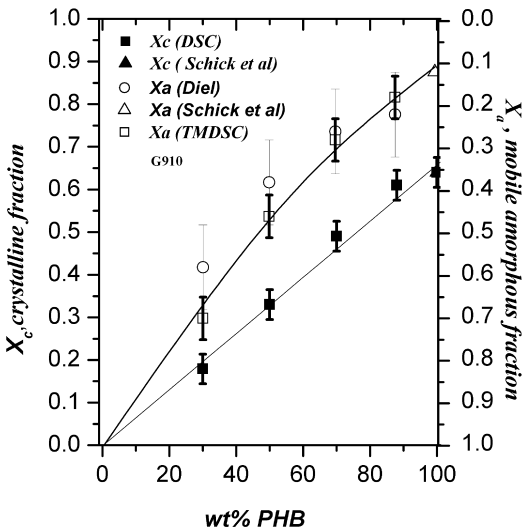

Fig. 10. Crystalline fraction X_c (left) and mobile amorphous fraction X_a (right) of blends of PHB with G910, crystallized at 80 °C for 3 h, in dependence on composition. The solid lines characterize the course of the functions as guide for the eye.

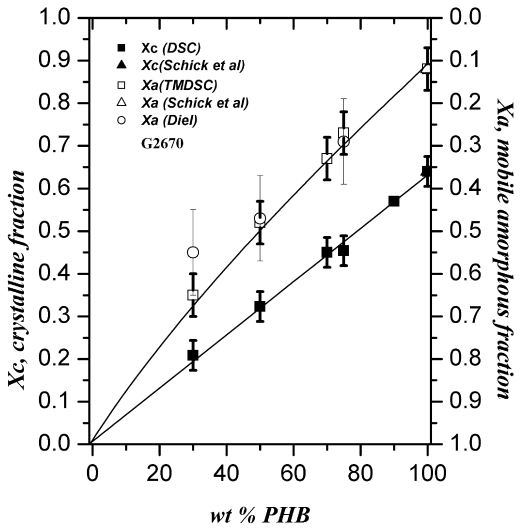

Fig. 11. Crystalline fraction X_c (left) and mobile amorphous fraction X_a (right) of blends of PHB with G2670, crystallized at 80 °C for 3 h, in dependence on composition. The solid lines characterize the course of the functions as guide for the eye.

crystals in its turn is strictly proportional to the PHB content (see Figs. 9–12). Under these circumstances the amount of the oligomer G910 or G2670 in the rigid amorphous phase is the difference between the total X_{ra} and the amount of PHB (i.e. the shadowed part in Figs. 12 and 13). These differences are included in Table 2 as fraction of G in the rigid amorphous phase (method I).

Another way to determine the composition of RAP starts from the measured T_g's of the mobile amorphous phase of the crystallized samples (Figs. 7 and 8) together with the assumption that the Fox equation [39] is valid for the T_g of

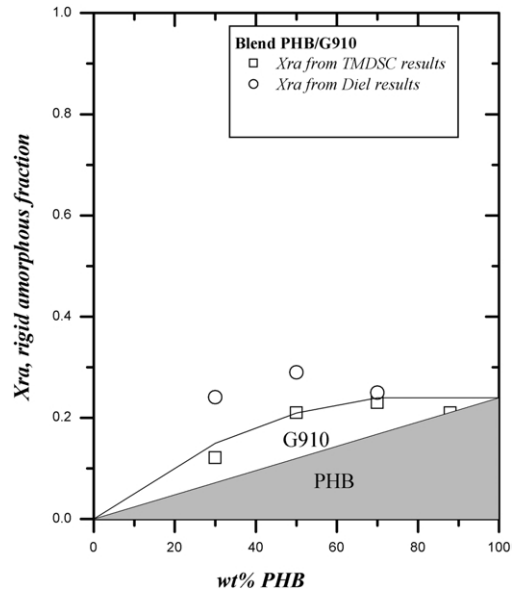

Fig. 12. Rigid amorphous fraction of different blends of PHB with G910 calculated from dielectric and TMDSC results using Eq. (1) and Fig. 10. The solid line is a guide for the eye only; the dashed area shows the linearly dependent amount of PHB in the RAP.

Table 2
Measured and calculated fractions of the different components in the different phases of blends of PHB with G 910 and G2670

Blends of PHB with	Crystalline fraction (X_c)	Mobile amorphous fraction (X_a)	Rigid amorphous fraction (X_{ra})	Fraction of *G* in rigid amorphous phase (method I)	T_g[a]/°C	Fraction of PHB in mobile amorphous phase	Fraction of G in mobile amorphous phase	Fraction of G in rigid amorphous phase (method II)
Pure PHB	0.64	0.12	0.24	0.00	−0	0.12	0.00	0.00
Blend with G910								
12% G910	0.61	0.19	0.20	0.00	−21	0.12	0.07	0.05
30% G910	0.49	0.27	0.24	0.07	−41	0.05	0.22	0.08
50% G910	0.33	0.45	0.22	0.10	−48	0.02	0.43	0.07
70% G910	0.18	0.67	0.15	0.08	−48	0.03	0.64	0.06
Blend with G2670								
10% G2670	0.57	0.18	0.25	0.03	−13	0.09	0.09	0.01
25% G2670	0.46	0.27	0.27	0.09	−18	0.09	0.18	0.07
30% G2670	0.45	0.33	0.22	0.05	n.d.	n.d.	n.d.	n.d.
50% G2670	0.32	0.48	0.20	0.08	−22	0.10	0.38	0.12
70% G2670	0.20	0.63	0.17	0.10	−24	0.12	0.51	0.19

[a] Weighted average from TMDSC and dielectric measurements on crystallized samples.

these blends. In this case the relative composition of the mobile amorphous phase (the PHB and the G content) can be derived from the measured T_g, that is to say, from the given ordinate (T_g) the respective abscissa is read from the fox curve which gives the amount of PHB in the mobile amorphous phase and thus, as the residue, even the G content in this phase (see Figs. 7 and 8 and Table 2). As a result the amount of *G* in the mobile amorphous phase turns out to be lower than the total amount of *G* in the blend (see Figs. 14 and 15 and Table 2). The difference must be the amount of *G* in the rigid amorphous phase; it is included in Table 2 as fraction of *G* in the rigid amorphous phase (method II).

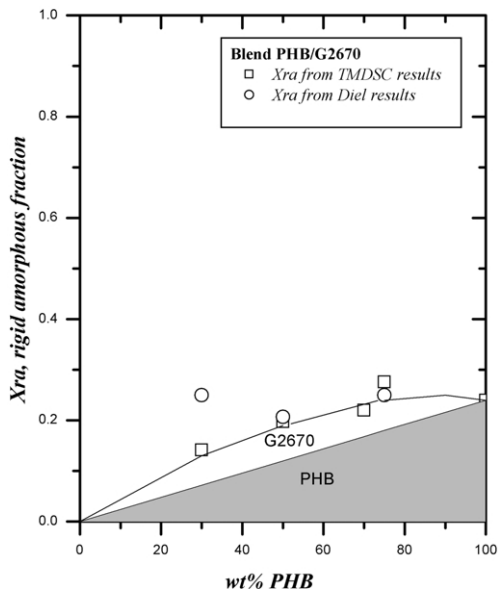

Fig. 13. Rigid amorphous fraction of different blends of PHB with G2670 calculated from dielectric and TMDSC results using Eq. (1) and Fig. 11. The solid line is a guide for the eye only; the dashed area shows the linearly dependent amount of PHB in the RAP.

As both methods give approximately the same result (see Table 2), we have to conclude that the above mentioned assumptions seem to be true and the evaluation useful. As a result, *G* is partially included in the rigid amorphous phase. The amount of *G* in the rigid amorphous phase is about 5–15% of the total mass of the sample. Though the results scatter somewhat it can be stated, that the fraction of *G* in the RAP depends somewhat on the molecular mass of the oligomer and, at least in the case of the higher molar mass component, even on the composition of the blend in question.

It may be of interest to mention that Chun et al. [7] reported, that for blends of PEEK with polyarylate the fraction of the rigid amorphous phase (relative to PEEK fraction) increased from 0.31 to 0.36 if the amount of polyarylate increases from 0 to 50%.

5. Conclusions

Blends of bacterial isotactic PHB with low molar mass atactic R, S-PHB-diols ($M_n = 910$, and 2670 g/mol) have been investigated relating to the rigid amorphous phase (RAP). The existence of this third phase, already proved for

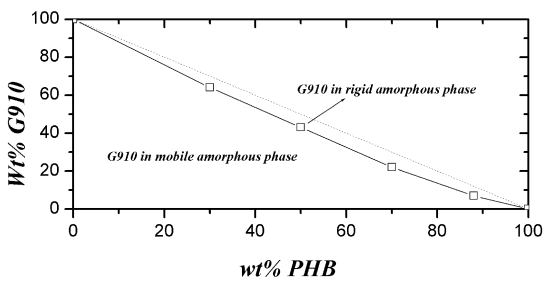

Fig. 14. Amount of G910 in the mobile amorphous phase as calculated from the glass transition temperature of the crystallized samples. The dotted line describes the total fraction of G910 in the blends.

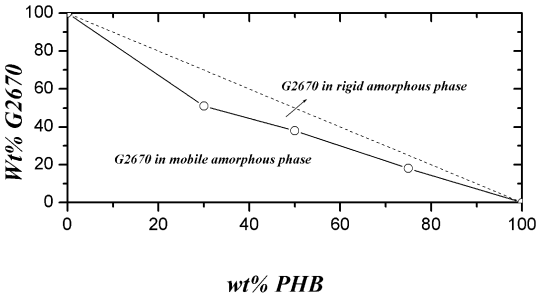

Fig. 15. Amount of G2670 in the mobile amorphous phase as calculated from the glass transition temperature of the crystallized samples. The dotted line describes the total fraction of G2670 in the blends.

pure bacterial PHB by other authors [10], could be confirmed even for the miscible blends with the named oligomers. It could be shown that the RAP contains mainly PHB but there is a small, but nevertheless significant, amount of the low molecular mass oligomer included in this interface which is thought to be situated between the crystals and the mobile amorphous phase. After crystallization of the samples, the low molecular mass oligomers are highly enriched in the mobile amorphous phase, which results in a decrease of the glass transition (lower for the low molecular mass oligomer), but some amount of the oligomers is incorporated in the RAP as well. The amount seems to be higher for the higher molecular mass oligomer. This is an interesting result which is important for the understanding of the bulk material properties and their change on blending PHB with oligomers. We believe that the rigid amorphous phase plays an important role in this context.

At this point the question arises, whether there is a relation between the amount and the composition of the rigid amorphous fraction on the one hand and the melting point depression, compared to pure PHB, of the blends on the other hand. There seems to be a connection, but to answer this question definitely, further investigations are needed.

Our findings from the PHB blends could furthermore contribute to a better understanding of the nature and properties of the rigid amorphous phase in general. The existence of the RAP even in blends is not widely known yet, but needs nevertheless more attention.

Acknowledgements

The authors are grateful to the DAAD (Deutscher Akademischer Austausch Dienst) for the grant given to Safaa H. El-Taweel, as well as to the Institut für angewandte Analysentechnik in Ulm, Germany for the possibility to perform the DSC measurements.

References

[1] Schick C, Wurm A, Mohammed A. Therm Acta 2003;396:119.
[2] Wunderlich B. Prog Polym Sci 2003;28:383.
[3] Toshihiko J, Shigeo A, Masao S. J Macromol Sci Phys B 1997;36:381.
[4] Cheng SZD, Wu ZQ, Wunderlich B. Macromolecules 1987;20:2802.
[5] Schick C, Donth E. Phys Scripta 1991;43:423.
[6] Schick C, Wigger J, Mischok W. Acta Polym 1990;41:137.
[7] Chun YS, Han Ys, Hyun JC, Kim WN. Polymer 2000;41:8717.
[8] Hong P-D, Chuang W-T, Yeh W-J, Lin T-L. Polymer 2002;43:6879.
[9] Schick C, Wurm A, Merzlyakov M, Minakov A, Marand H. Therm Anal Calorimetry 2001;64:549.
[10] Schick C, Wurm A, Mohammed A. Colloid Polym Sci 2001;279:800.
[11] Huo P, Cebe P. Macromolecules 1992;25:902.
[12] Cheng SZD, Cao My, Wunderlich B. Macromolecules 1986;19:1868.
[13] Lovinger AJ, Hudson SD, Davis DD. Macromolecules 1992;25:1992.
[14] Santa Cruz C, Stribeck N, Zachmann HG, Balta Calleja FJ. Macromolecules 1991;24:5980.
[15] Sauer BB, Hsiao BS. Polymer 1995;36:2553.
[16] Doi Y. Microbial polyesters. New York: VCH; 1990. Chapter 1.
[17] Grassie N, Murray EJ, Holmes PA. Polym Degrad Stab 1984;6:47.
[18] Dekoning GJM, Lemstra PJ. Polymer 1992;33:3295.
[19] Dekoning GJM, Lemstra PJ. Polymer 1993;34:4089.
[20] Biddelstone F, Harris A, Hay JN, Hammond T. Polym Int 1996;39:221.
[21] Ha C-S, Cho W-J. Prog Polym Sci 2002;27:759.
[22] Greco P, Martuscelli E. Polymer 1989;30:1475.
[23] Abe H, Doi Y. Macromolecules 1996;29:8683.
[24] Abe A, Matsubara I, Doi Y, Hori Y, Yamaguchi A. Macromolecules 1994;27:6018.
[25] Pearce R, Jesudason J, Orts W, Marchessault RH, Bloembergen S. Polymer 1992;33:4647.
[26] Pearce R, Brown GR, Marchessault RH. Polymer 1994;35:3984.
[27] Saad GR. Polym Int 2002;51:338.
[28] Paglia D, Beltrame E, Canetti PL, Seves A, Marcandalli B, Martuscelli E. Polymer 1993;34:996.
[29] Sadocco P, Canetti M, Seves A, Martuscelli E. Polymer 1993;34:3368.
[30] Neuenschwander, et al., US. Patent, 1997, Nr. 5665831.
[31] Saad GR, Lee YJ, Seliger H. Macromol Biosci 2001;1:91.
[32] Höhne G, Hemminger W, Flammersheim HJ. Differential scanning calorimetry, 2nd (enlarged) ed. Berlin: Springer; 2003.
[33] Hensel A, Dobbertin J, Schawe JEK, Boller A, Schick C. Therm Anal 1996;46:935.
[34] Hensel A, Schick C. J Non-Cryst Solids 1998;235:510.
[35] Theobald S, Pechhold W, Stoll B. Polymer 2001;42:289.
[36] Heinrich B, Stoll B. Progress Colloid Polym Sci 1988;78:37.
[37] Scholl HU, PhD Thesis, University of Ulm; 2001.
[38] Heinrich W, Stoll B. Colloid Polym Sci 1985;263:873.
[39] Fox TG. Bull Am Phys Soc 1956;1:123.
[40] Okohoshi I, Abe H, Doi Y. Polymer 2000;41:5985.
[41] Focarete ML, Ceccorulli G, Scandola M, Kowalczuk M. Macromolecules 1998;31:8485.
[42] Böttcher CJF. Theory of electric polarization. Amsterdam: Elsevier; 1973.
[43] Barham PJ, Keller A, Otun EL, Holmes PA. J Mater Sci 1984;19:2781.
[44] Lee HS, Kim WN. Polymer 1997;38:2657.